A Comparison of Month-to-Month Persistence of Anomalies in a General Circulation Model and in the Earth's Atmosphere

HUUG M. VAN DEN DOOL

Department of Meteorology, University of Maryland, College Park, MD 20742

ROBERT M. CHERVIN

National Center for Atmospheric Research, Boulder, CO 80307*

(Manuscript received 11 October 1985, in final form 3 February 1986)

ABSTRACT

The output of a 20-year integration of an annual cycle (AC) version of the NCAR Community Climate Model in which the external conditions went through 20 prescribed identical annual cycles is used to study month-to-month persistence of anomalies in monthly mean atmospheric circulation fields on a global and a hemispheric scale. Of all fields considered, the height fields (1000–300 mb) are the most persistent and the transient eddy flux fields the least persistent. Persistence in height field anomalies is largest in winter and small throughout the rest of the year. For the area north of 20°N, a comparison is made with the persistence of monthly mean height and temperature fields observed in the real world (RW) during a 28-year interval. On a pooled all month-pairs basis, RW height anomaly fields are significantly more persistent than those appearing in AC but, from a practical point of view, the difference is small. The differences in persistence are larger for temperature anomalies (500–1000 mb thickness) than for height. Differences between RW and AC monthly persistence over the area north of 20°N are largest in summer when the RW has a local maximum in persistence. On the assumption that the model and atmosphere have the same internal dynamics, the differences just described can be attributed to the interaction of the atmosphere with external or boundary conditions (e.g., ocean surface temperatures), which was purposely omitted from the AC integration. Interaction with the lower boundary in summer seems, therefore, to be quite important to explain the observed level of month-to-month persistence in circulation anomalies. In winter, however, the internal dynamics of the atmosphere alone produces the required observed level of month-to-month persistence. The output of a 15-year integration of the same model in which the sea surface temperature, on a global scale, had realistic interannual variability, is used to interpret further the differences between RW and AC.

As a by-product of this study we have calculated the spatial degrees of freedom (dof) associated with time mean anomaly fields. The dof for global monthly mean anomaly height fields in the AC model are quite low, i.e., 25–35 on a yearly pooled basis. Over the area north of 20°N, the dof associated with monthly mean anomaly height fields of the AC model and the RW are quite close, varying from 15–20 in winter months to about 40 in summer.

1. Introduction

Although the frictional and radiational damping time scales of the earth's troposphere are supposed to be only 5 to 10 days, there appears to be a substantial level of variability at time scales longer than 10 days (see, for example, Blackmon et al., 1984). According to Blackmon et al., there are vast areas in the Northern Hemisphere where more than half of the total variance in the winter 500-mb height field passes through a 30-day mean time filter.

There may be two complementary reasons for low-frequency variability. First of all, the dynamics may produce free instabilities of sufficient growth rate and low enough frequencies (Simmons et al., 1983); secondly, forcing by persistent anomalous features at the earth's surface may determine the time scale of forced anomalous flow in the atmosphere. The relative role of these factors is the subject of many studies and is intimately related to the question whether or not there exists, at long time scales, dynamic predictability (Shukla, 1981), predictability due to lower-boundary forcing (Opsteegh and Van den Dool, 1980) or a combination of both.

One strategy to isolate the influence of the lower boundary would be to run a credible atmospheric model in two different modes. In the first mode, the boundary conditions are specified and fixed at their normal values; in this run only the dynamics can be made responsible for variance at low (or any) frequency. In the second mode, the lower boundary is changing interactively, thereby potentially forcing anomalies in the atmosphere at time scales typical for

* The National Center for Atmospheric Research is sponsored by the National Science Foundation.

the lower boundary (e.g., a few months for the ocean's surface temperature anomalies). However, since fully coupled global ocean/atmosphere models are still in the rudimentary development stage, we will replace the second mode by a suitable set of observations of the real world. This substitution has the potential disadvantage that we may study not only the differences caused by possibly different treatment of the lower boundary but also differences caused by different dynamics of the model (compared to the real world). For the purpose of this study, we assume that the model internal dynamics and the persistence it produces are the same as in the real atmosphere.

In this paper we will concentrate on one particular aspect of low frequency variability, namely, month-to-month autocorrelation of anomalies in monthly means. Anomalies are defined as the departure of an individual monthly mean from a long-term mean for that month. The study of this type of persistence has a long tradition (see Namias, 1952, for example), mainly because it pertains directly to the practical prediction question. Here we examine month-to-month persistence in conjunction with ongoing efforts to compare the interannual variability of monthly or seasonal means in models to the real world (Manabe and Hahn, 1981; Chervin, 1986). For certain conditions there is a close correspondence between the variability of time means and the lag correlation of time means. Assume, for example, that the monthly mean anomaly of x (i.e., $\bar{x}$) is governed by a stationary process given by

$$\bar{x}_{i+1} = \rho \bar{x}_i + \epsilon_i \tag{1}$$

where i is the month's number, ρ is month-to-month correlation (independent of i), the expected value of $\bar{x}$, $\langle \bar{x} \rangle$, is zero and ϵ_i is a random number with $\langle \epsilon_i \rangle = 0$ and $\langle \epsilon_i^2 \rangle = \sigma^2$. It is easy to see that the variance of $\bar{x}$ is given by

$$\langle \bar{x}_i^2 \rangle = \sigma^2/(1 - \rho^2). \tag{2a}$$

In other words, the larger ρ the larger $\langle \bar{x}_i^2 \rangle$ and vice versa (leaving σ^2 unchanged), a result which, at first sight, seems to be counterintuitive. This enigma can be explained by the realization that although a high level of month-to-month persistence will necessarily reduce the variability within a season, more extreme monthly anomalies become possible with large ρ, and hence, large interannual variability can be achieved. Of course, $\bar{x}$ may not quite be governed by (1) and to that extent autocorrelation and variance provide complementary information.

Strictly speaking, (1) applies to a set of sequential months. In the real world ρ and ϵ are likely to be seasonally dependent and (1) is no longer a stationary process. Therefore, it seems necessary to stratify the data by the calendar month (m) and to study variability of $\bar{x}_i$ for each month separately. One may still think of $\bar{x}_i$ generated by

$$\bar{x}_{i+1} = \rho_m \bar{x}_i + \epsilon_{i,m} \tag{1a}$$

where m cycles through the integers 1–12, and ρ_m and $\epsilon_{i,m}$ are now a function of m. The variant of (2a) then takes the form

$$\langle \bar{x}_{i+1}^2 \rangle = \rho_m^2 \langle \bar{x}_i^2 \rangle + \sigma_m^2 \tag{2b}$$

where $\langle \ \rangle$ refers to the expected value for $i = m$, $m + 12$, $m + 24$, $\cdots$, i.e., the interannual variability of the monthly means separately for each month m, $m = 1, 2, \cdots, 12$. To the extent that $\langle \bar{x}_i^2 \rangle$ does not change too much from m to $m + 1$, (2a) remains valid and therefore large autocorrelation implies large interannual variability. Obviously (2a) is more valid in summer and winter (when ρ and σ vary little) than in spring and fall, and for lags longer than 1 month (2a) loses its applicability.

In this paper we study the level of month-to-month persistence of monthly mean atmospheric anomalies both in the real world (RW) and in an extended run of an annual cycle version of the Community Climate Model (CCM) developed at the National Center for Atmospheric Research in Boulder (see Chervin, 1986, for details). The model data are derived from a 20-year annual cycle (AC) run in which solar insolation, sea surface temperature (SST), sea ice and snow cover go through identical prescribed annual variations each year. In this experiment only the internal dynamics of the model can produce low-frequency variance. None of the surface fluxes feed back on the state of the ocean surface.

Subsection 2a will describe the RW data, as well as (briefly) the model that produced the AC data. In subsection 2b, definitions are given for pattern correlation and temporal correlation coefficients which will both be used as measures of month-to-month persistence. We will also discuss there a method to estimate the number of spatial degrees of freedom from the standard deviation of the pattern correlation coefficient. The results in a yearly pooled sense will be discussed in subsection 3a. In subsection 3b–3c, we present the seasonal aspects and cases of extreme persistence in the model. The geographical distributions of month-to-month persistence based on AC and RW are presented in subsection 3d and autocorrelation at lags longer than 1 month in the AC data is discussed in subsection 3e.

Both the overall level of persistence and the seasonality of persistence (in the model) enable us to test (reject, accept or improve) the explanation for month-to-month persistence in the real world as proposed by Van den Dool (1983). In that paper all emphasis was on the stationary atmospheric response to steady anomalous forcing. The idea is that for long enough time scales the atmosphere is in equilibrium with steady anomalous forcing and therefore the cause of persistence in the atmosphere should be in the presence of such steady anomalous forcing. Since the AC run has no steady anomalous forcing we have to expect that in this model the level of persistence is lower than that in the real world. The seasonality in month-to-month persistence was explained in Van den Dool (1983) from

linear dynamic theory. The atmospheric stationary response to steady anomalous forcing was found to be most persistent when the climatological background flow changes least, which is from January to February and July to August. In the AC run, there is no reason to expect such a seasonality since there is no steady anomalous forcing.

2. Data and analysis

a. Data

We will use or refer to results of calculations based on many different data sets. On the observational side, we have 33 years of monthly mean 700 mb heights based on twice daily analyses made at the National Meteorological Center, Washington, DC. The period is January 1949–January 1982 and we will use data available north of about 20°N. All results based on this data set to be discussed in the present paper can more extensively be found in Van den Dool and Livezey (1984). We will also use 28.5 years of monthly mean 500 mb, sea level pressure and 500–1000 mb thickness maps based on daily analyses provided by the German Meteorological Service at Offenbach (FRG). This period is January 1949 to July 1977, the area is north of 20°N (data coverage not complete in the earlier years) and most of the results based on this data set have already been published (Van den Dool, 1983). Together these two data sets give an impression of the lower troposphere in the subtropical to high latitudes of the Northern Hemisphere; these two data sets will, nevertheless, loosely be referred to as the real world (RW).

On the General Circulation Model output side, we have a 20-year annual cycle (AC) run. The version of the Community Climate Model used to generate the data is described in Chervin (1986). The model has global coverage, nine σ-layers in the vertical, a rhomboidal resolution truncated at wavenumber 15, and interactive clouds. All external factors (solar radiation, SST, snow and sea ice cover, chemical composition of the atmosphere) went through 20 prescribed identical annual cycles. Over the oceans the surface temperature is prescribed (infinite thermal inertia); over land (and sea ice) the surface temperature is calculated from an energy balance equation in which the thermal inertia is set equal to zero. The details about the original CCM can be found in Pitcher et al. (1983) and references thereof. The following AC data were used: 20 years of anomalous monthly mean distributions of many variables (at various levels) on a 48 by 40 longitude/latitude grid. The particular fields we will study here are listed in Table 1. All data were detrended; i.e., for each monthly mean quantity, each level and each grid point a straight line (a least-squares fit to 20 data points) was subtracted from the AC data. Of all the quantities listed in Table 1 we can use only the height fields for a pertinent comparison to RW data and for the restricted area of $\phi \geq 20°$N only. For all other quantities and areas we have just the model output.

One difference in treatment of AC and RW data has to be mentioned here. The AC data were detrended while the RW data were not. Further analysis of RW data over the period 1963–77 (not shown here) shows that the results to be discussed in the present paper are insensitive to detrending the RW data; furthermore, results for 1963–77 and 1949–82 are quite close.

b. Analysis

There are (at least) two ways to express the degree of similarity in anomaly patterns occurring in adjacent months, namely, the pattern correlation (PC) and the temporal correlation (TC).

A temporal correlation between time series X and Y can be defined by

$$\mathrm{TC}_{n,m,\tau}(X, Y) = \frac{\frac{1}{N}\sum XY - \frac{1}{N^2}\sum X \sum Y}{\left\{\left[\frac{1}{N}\sum X^2 - \frac{1}{N^2}(\sum X)^2\right]\left[\frac{1}{N}\sum Y^2 - \frac{1}{N^2}(\sum Y)^2\right]\right\}^{1/2}} \tag{3}$$

where X and Y are defined on N points in time and the summation is over N points in time; the indices n, m and τ refer, respectively, to a particular grid point in space, a particular month and the lag separating the two time series (in units of months). For example, selecting 20 Januaries and 20 Februaries ($m = 1$, $\tau = 1$) monthly mean 500 mb heights at 50°N, 0°W (n) yields two time series from which $\mathrm{TC}_{n,1,1}$ can be calculated. In summary, a TC is a function of month, lag and the position in space.

An alternative way is to employ the pattern correlation

$$\mathrm{PC}_{j,m,\tau}(X, Y) = \frac{\frac{1}{W}\sum w_n XY - \frac{1}{W^2}\sum w_n X \sum w_n Y}{\left\{\left[\frac{1}{W}\sum w_n X^2 - \frac{1}{W^2}(\sum w_n X)^2\right]\left[\frac{1}{W}\sum w_n Y^2 - \frac{1}{W^2}(\sum w_n Y)^2\right]\right\}^{1/2}}, \tag{4}$$

TABLE 1. Description of monthly mean anomalies extracted for further analysis from the 20-year AC run.

Quantity	Level (mb)	Symbol
Zonal wind	300	U3
Temperature	700	T7
Meridional flux of zonal momentum by transient eddies	300	CUV3
Meridional flux of temperature by transient eddies	850	CVT85
Standard deviation of zonal wind within the month	300	SU3
Standard deviation of meridional wind within the month	300	SV3
Height	950	Z95
Height	700	Z7
Height	500	Z5
Height	300	Z3
Energy flux at earth atmosphere interface		ENETS

where X and Y are each defined on a spatial grid on time levels separated by a lag τ, the summation is over space, w_n is a weight for the area represented by the nth gridpoint [w_n = cos (latitude)], $W = \Sigma\, w_n$, and the indices j, m, τ stand for the year, month and lag, respectively. For example, selecting the January and February 500 mb height fields on a global scale in year 1, one can calculate $PC_{1,1,1}$. The PC is a function of year, month and lag.

The PC and TC are theoretically close if we average PC over all years and TC over all gridpoints, provided that we put w_n equal to 1 everywhere and provided further that there are no trends (in time) in the data. At each grid point a linear trend line was calculated and subtracted from the AC data. This cures the trend problem to a large extent but since it is arbitrary to assume that the trend is linear—or anything else—some doubt will continue to be cast on the TC calculation. The PC is much less sensitive to trends and actually changes very little from raw to detrended data.

Since we have calculated a large number of correlation coefficients, say $PC_{j,1,1}$ (Z5, Z5) for $j = 1, 20$, we can consider the distribution of these coefficients. For an expected value $\langle PC \rangle = 0$ and normally distributed PC's, the standard deviation of the PC's should obey (Panofsky and Brier, 1968)

$$\text{sd} = (N_e - 2)^{1/2}, \tag{5}$$

where N_e is the number of spatially independent grid points or the degrees of freedom (dof). Since we can calculate a sample value of sd we will infer from (5) what N_e apparently is and derive in this indirect way important climatological information about the typical spatial scale of anomalies appearing on either observed or model-generated monthly mean anomaly maps. As we will see below, $\langle PC \rangle \approx 0.1$ rather than 0 but 0.1 is small enough to derive estimates of dof from (5). It should be pointed out that dof is not uniquely defined and in this case it has its meaning in connection with the "standard error" of estimate of a correlation coefficient. Other definitions of dof are possible in connection with standard errors of other quantities.

The PC can be analyzed over any given domain and we will show results for four different areas, namely, 1) global, 2) $\phi \geq 20°$N, 3) Northern Hemisphere (NH), and 4) Southern Hemisphere (SH). Area 2 is the one where we can make a comparison with observational studies, and we will therefore pay most of the attention to that area in the remainder of the paper.

3. Results

a. *Yearly pooled results of AC run*

For each quantity (U3, . . . , ENETS) and for each area (1, . . . , 4) there are 239 pairs of adjacent ($\tau = 1$) monthly mean anomaly patterns that can be compared using the PC. Ignoring all seasonality in the results, Table 2 gives for each quantity and each area the average (ave) of the PC (over 239 cases), the standard deviation (sd) of individual PC's around the mean, and the implied degrees of freedom (dof) using (5).

As can be seen from Table 2 all PC's are positive on average for all areas and quantities. Evidently, the internal dynamics of the CCM produces a certain degree of persistence in anomalies on the monthly time scale. However, the level of persistence is quite low and never exceeds $\overline{PC} = 15\%$. The results seem to be fairly consistent from one area to the next. We hesitate to attribute much significance to the fact that anomalies in the CCM's Southern Hemisphere are more persistent than in the Northern.

Stratifying the quantities in decreasing order of persistence, one finds Z95, Z7, Z5, Z3, U3, T7 as somewhat persistent and CUV3, CVT85, SU3, SV3 and ENETS as least (virtually not) persistent. This is a curious result because within the framework of steady state modeling the latter group represents forcing terms, whereas the former group represents response quantities. Apparently it is possible to have persistence in height field anomalies without the forcing being the controlling factor in determining the time scale of these height field anomalies. This clearly points to the internal dynamics being responsible for at least part of the low-frequency variability in the CCM and by implication one is forced to wonder whether this may also be true in the RW.

The question arises whether the average PC's differ significantly from zero. Our a posteriori test is clarified by the following example. For Z3 we find $\overline{PC} = 12.41$ and sd = 16.92 for area 1 (globe); see Table 2. Therefore the sd of the mean PC should be sdm = $16.92/\sqrt{239} = 1.09$ assuming further that the 239 PC's are independent. Clearly 12.41 is a large number of sdm's away from zero. Following this procedure we have marked (with an asterisk) all $\overline{PC}$'s in Table 2 that are two or more sdm's away from zero. There can be little doubt

TABLE 2. Pattern correlations (%) at 1 month lag for anomalies in monthly mean patterns of various quantities occurring in the AC run. For each area and each quantity the average (over 239 cases), the standard deviation and the implied degrees of freedom are given. Values refer to year-round results.

Area	Quantity	U3	T7	CUV3	CVT85	SU3	SV3	Z95	Z7	Z5	Z3	ENETS
Globe	ave	8.99*	7.59*	1.51*	0.69	1.37*	3.12*	12.59*	12.94*	12.22*	12.41*	4.07*
	sd	12.87	12.42	5.61	9.59	6.11	6.76	19.55	19.74	18.10	16.92	10.59
	dof	62.33	66.85	319.74	110.68	269.61	220.66	28.16	27.66	32.52	36.92	91.14
$\phi \geq 20°N$	ave	8.02*	7.85*	0.67	1.25	0.89	3.69*	8.56*	9.55*	9.43*	9.68*	4.48*
	sd	19.03	17.81	9.64	11.45	9.93	11.80	24.51	24.95	23.21	23.21	16.47
	dof	29.60	33.53	109.52	78.22	103.41	73.80	18.64	18.07	20.56	20.56	38.86
Northern	ave	8.04*	8.23*	0.72	1.17	0.99	3.07*	9.45*	10.04*	9.54*	10.31*	3.98*
Hemisphere	sd	16.56	17.29	8.22	11.13	8.43	9.64	23.64	24.31	23.23	23.43	13.76
	dof	38.48	35.45	150.00	82.75	142.83	109.62	19.89	18.92	20.54	20.21	54.83
Southern	ave	9.50*	6.68*	2.56*	0.75	1.79*	3.14*	14.78*	14.92*	13.94*	13.74*	3.73*
Hemisphere	sd	15.51	14.27	7.64	10.58	7.95	8.67	25.06	25.51	23.39	21.75	11.30
	dof	43.57	51.12	173.31	91.27	160.41	135.16	17.93	17.37	20.28	23.15	80.30

* Differ more than two standard deviations (standard deviation of average over 239 cases) from zero.

that the height, temperature and wind fields have nonzero 1 month autocorrelation. To the extent that the 239 PC's are not independent, sdm will be larger but probably not large enough to invalidate the above conclusions.

The dof N_e implied by (5) are surprisingly small. Even on a global scale there are only 25–35 dof in monthly mean height fields. This reflects the large spatial extension of height anomalies at all levels. More "spotty" fields such as the eddy momentum flux seem to have several hundreds of dof associated with them. Note that dof are not strictly additive; dof for the Northern and Southern hemispheres do not add up exactly to dof for the globe. This result is a consequence of the fact that the two hemispheres are not independent.

In Van den Dool (1983), calculations identical to the ones given herein but based on RW data were discussed. In Table 3 the appropriate comparison between RW and AC is made for Z5, Z95 (sea level pressure in Van den Dool) and thickness Z5–Z95 (Z5–Z10 in Van den Dool); the area is $\phi \geq 20°N$. In view of the argument put forward in the Introduction, it is reasonable to expect more persistence in the RW than in the AC run. This turns out to be the case for all three quantities studied, most convincingly so for the thickness patterns (20% in RW versus 7% in AC). Taking conservative values for sd (25) and the number of independent cases (200), we note that the difference between two mean PC's has an expected value of 0 (null hypothesis) and a standard deviation sdd = $25\sqrt{2}/\sqrt{200} = 2.5$. Applying a one sided t-test, the difference in PC for AC and RW is significant at the 5% level for the height fields and highly significant (<0.5% level) for the thickness fields. Nevertheless, from a practical point of view it is fair to say that height anomalies in the AC run are hardly less persistent than those in the real world.

One may argue that taking straight averages over a collection of 239 correlation coefficients is not the appropriate thing to do. (See Faller, 1981, for example.) An alternative may be to consider a summation over explained variance retaining sign;

$$\overline{PC^2} \equiv \frac{1}{239}\sum_{i=1}^{239} PC_i abs(PC_i) \tag{6a}$$

and to subsequently take a square root while maintaining the sign. Since the PC_i's are close to zero this procedure yields PC only a little higher than that obtained from

$$\overline{PC} = \frac{1}{239}\sum_{i=1}^{239} PC_i. \tag{6b}$$

Moreover (6a) is arbitrary in its own way and it is no longer obvious how to infer dof. Therefore, we discuss results based on straight averages while realizing that this procedure gives a conservative impression of the true autocorrelation.

b. Seasonality

Figure 1 shows the degree of persistence in Z5, Z95 and Z5–Z95 over the area north of 20°N as a function

TABLE 3. Average pattern correlation for the area $\phi \geq 20°N$ at 1 month lag for the AC and RW runs. [The third column gives the difference of AC and RW expressed in units of standard deviation (of the difference between two means); i.e., the Student's t quantity.] Values are for the whole year.

	AC		RW		
Quantity	ave	sd	ave	sd	(AC − RW)/sdd
Z5	9.4	23	14.0	22	1.8*
Z95 (p_{sl})	8.6	25	13.0	23	1.8*
Z5–Z95 (Z5–Z10)	6.9	19	20.0	20	5.2*
Total cases	239		342		

* Significance of the one-sided t-test at the 5% level.

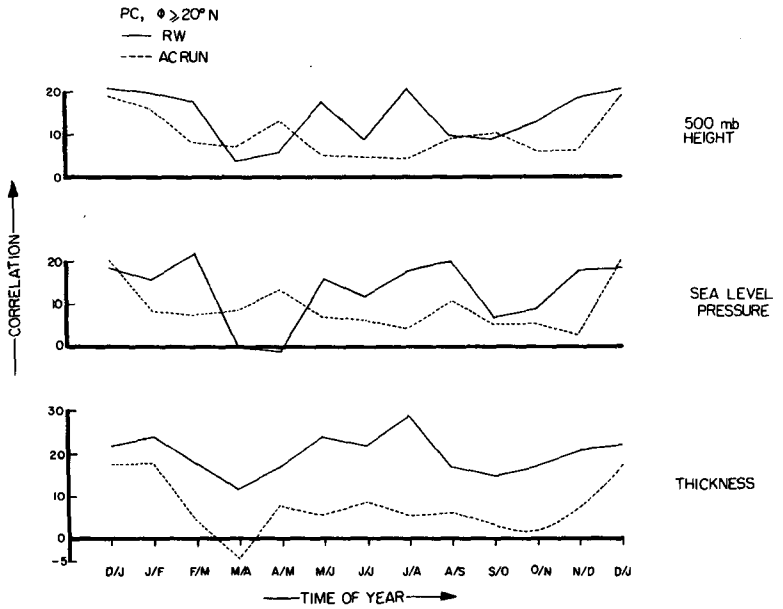

FIG. 1. Month-to-month pattern correlation coefficients (in percentage) of anomalies in monthly mean fields of 500 mb height (Z5); surface pressure (p_{sl} or its proxy Z95) and 500–1000 mb thickness (Z5–Z10, or its proxy Z5–Z95) as a function of the time of year. The solid line refers to the real world (RW), the dashed line to the annual cycle GCM run (AC). The area considered is $\phi \geq 20°$N. The graphs represent averages over 29 individual cases in the RW (1949–77) and averages over 20 individual cases in the AC (20 model years).

of season for both the AC run and the RW. For each pair of months, 20 individual PC values are averaged pertaining to the AC run (dashed line). The RW graphs (solid line) show the averages over 29 cases. It is immediately clear that for all three quantities considered the AC run has little persistence throughout most of the year ($5 < \overline{PC} < 10$) and it is only in winter that the $\overline{PC}$ reaches values of about 20. In contrast, the RW curves have two maxima, one in summer and one in winter, both of which are broad and not very much peaked. In all months of the year, thickness anomaly patterns in RW are more persistent than in AC, the difference being largest in summer. In 9 out of 12 months, sea level pressure and 500 mb height anomalies are more persistent in RW than in AC. Figure 1 yields strong evidence that indeed there is more persistence in RW than in AC, especially in summer and in temperature fields. Therefore, we are inclined to believe that, indeed, interaction with the lower boundary is needed to fully explain the month-to-month persistence in RW. However, in winter and in the height fields in particular the dynamics of the CCM alone are sufficient to explain the level of persistence observed in RW. Although these conclusions seem straightforward, of course, they lose their validity if the dynamics of the CCM and the RW are different.

Table 4 gives more quantitative information on the difference between AC and RW. For each pair of months one can find the average, the standard deviation, the implied dof according to (5) and the difference of RW and AC expressed in the standard deviation of the difference between two means. The latter quantity is formed to apply a t-test and the asterisks are used to denote that persistence in the RW is significantly (at the 5% level according to the one sided t-test) larger than in the AC. As can be seen, RW height fields are significantly more persistent in only 4 out of 12 months while the RW thickness fields are significantly more persistent in 10 out of 12 months, the difference being most impressive in summer.

An interesting feature of Table 4 is that the standard deviations of the PC in the AC run and the RW are quite close and show the same dependence on season. Converted via (5) into dof, this implies that, both in the model and in the RW, height anomalies north of 20°N have more dof in summer (up to 40) than they have in winter (down to 15). This agreement gives credence to the capability of the CCM to generate monthly mean anomalies of the right spatial scale. Our calculation of dof for monthly mean data are in fair agreement with Livezey and Chen (1983) who found around 35 (55) dof to be associated with RW winter (summer) seasonal mean 700 mb height for the area north of 20°N.

c. *Extreme cases of (anti) persistence*

Figure 2 shows the highest and the lowest pattern correlation over the area $\phi \geq 20°$N as a function of season that occurred during the record of 20 AC and

TABLE 4. The month-to-month pattern correlation (%) of anomaly patterns in the 500 mb height, surface pressure, and thickness. The correlation is determined for the area north of 20°N. The four rows per item contain the average over all years, the standard deviation relative to that average, the spatial degrees of freedom inferred from Eq. (5) and the difference between RW and AC expressed in units of standard deviation of the difference between two means.

		Jan/Feb	Feb/Mar	Mar/Apr	Apr/May	May/Jun	Jun/Jul	Jul/Aug	Aug/Sep	Sep/Oct	Oct/Nov	Nov/Dec	Dec/Jan
						Z_{500}							
$\overline{PC}$	RW	20	18	4	6	18	9	21	10	9	13	19	21
	AC	16	8	8	13	6	5	5	9	11	6	7	19
sd	RW	28	20	24	17	20	19	20	21	27	24	29	
	AC	30	20	26	21	16	18	19	22	28	24	30	
dof	RW	15	27	20	36	27	37	30	28	24	16	20	14
	AC	16	25	41	42	33	31	22	15	19	14	13	27
$\frac{RW-AC}{sdd}$		0.5	1.7*	−0.5	−1.3	2.2*	0.8	2.9*	0.2	−0.3	0.9	1.7*	0.2
						$p_{surface}$ (Z_{950})							
$\overline{PC}$	RW	16	22	0	−1		12	18	20	7	9	18	19
	AC	9	8	9	14	16 7	6	5	11	6	6	3	20
sd	RW	29	21	25	20	24	17	25	17	21	21	25	29
	AC	34	27	29	23	18	17	20	16	17	25	27	28
dof	RW	14	25	18	27	19	38	19	36	25	25	18	14
	AC	14	20	33	35	6	42	35	18	16	15	11	16
$\frac{RW-AC}{sdd}$		0.9	2.0*	−1.1	−2.4	1.4	1.2	1.9*	1.9*	0.2	0.5	2.1*	−0.1
						Z_{500}–Z_{1000} (Z_{500}–Z_{950})							
$\overline{PC}$	RW	24	18	12	17	24	22	29	17	15	17	21	22
	AC	18	5	−5	8	6	9	6	6	4	2	7	18
sd	RW	27	22	21	15	17	17	16	18	19	25	25	22
	AC	21	19	17	14	14	17	14	15	20	22	20	23
dof	RW	16	23	24	45	37	38	41	34	29	18	17	
	AC	24	30	35	50	52	36	55	48	29	22	28	
$\frac{RW-AC}{sdd}$		0.8	2.1*	2.9*	2.1*	3.8*	2.6*	5.1*	2.3*	1.8*	2.1*	2.1*	0.6
number of years	RW	29	29	29	29	29	29	28	28	28	28	28	28
	AC	20	20	20	20	20	20	20	20	20	20	20	20

* Significance at the 5% level of the one sided *t*-test.

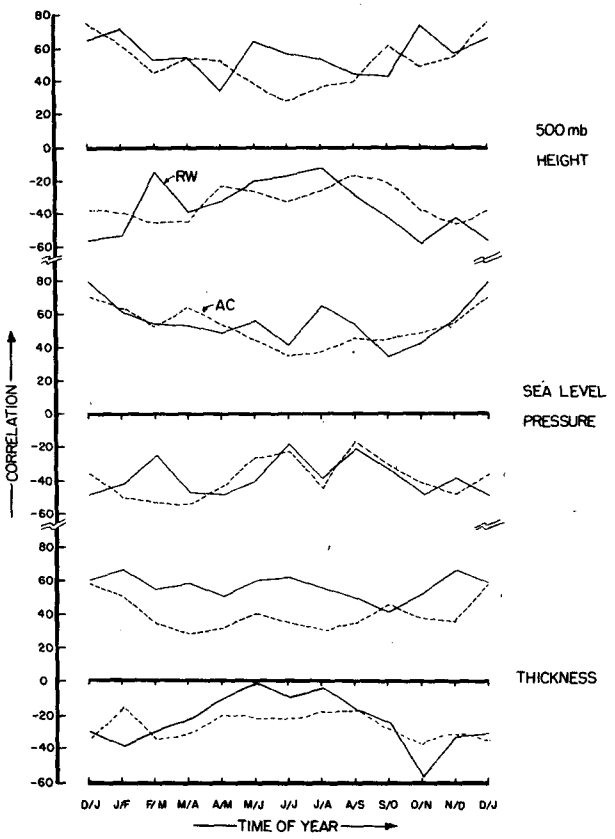

FIG. 2. As in Fig. 1 except the highest and the lowest pattern correlation found in the RW (solid line) and AC (dashed line) run.

28 RW years. Both the RW and the AC run produce individual cases of remarkable persistence (~70) and anti-persistence (~ −60). In agreement with the seasonality of the standard deviation (see Table 4) the values in Fig. 2 deviate farther from zero in winter than they do in summer. For all quantities considered, 500 mb height, sea level pressure and thickness, extreme persistence is higher than (in absolute value) extreme antipersistence, which indicates a small shift of the entire frequency distribution of PCs towards positive values. This shift is particularly clear in the RW thickness curves and, in fact, negative PCs in summer have hardly been observed, which is a strong indication of the importance of long time scales in the RW summer thickness fields.

It is hard to see any systematic differences between the AC and RW curves in Fig. 2, at least for 500 mb and sea level pressure. In other words, extreme persistence or antipersistence in AC is not very different from that in RW. This agrees with our earlier conclusion that persistence in RW, from a practical point of view, is not much higher than it is in the AC. However, the differences between RW and AC show up quite clearly again in the thickness fields. In nearly all months extreme persistence in the RW for thickness is stronger than in AC while extreme antipersistence in RW is weaker than in AC.

It is of some interest to display the geographical patterns of the most persistent anomalies in the AC run. Figure 3 shows the 500 mb anomalies in the December and adjacent January leading to PC = 76% for the area $\phi \geq 20°$N. One may speculate that in this case a mode of sufficient growth rate and low enough frequency has been excited, although the anomalies shown in Fig. 3 do not resemble any of the more unstable modes discussed in Simmons et al. (1983) for a barotropic model. The major contribution to the autocorrelation in Fig. 3 seems to come from zonally symmetric anomalies, a seesaw between high and lower Northern Hemisphere latitudes. Further inspection of all cases satisfying PC $\geq$ 50 for 500 mb height anomalies over the area $\phi \geq 20°$N (11 cases, almost all of them in the winter season and 4 of them D/J) reveals that in the majority of cases the zonally symmetric north–south seesaw was pronounced and (obviously) persistently present. It is worth pointing out that the first empirical orthogonal function of RW seasonal mean 500 mb winter data (Lau, 1981) and the regime average of quasi-stationary daily 500 mb height data (Horel, 1985) do show a very similar north–south seesaw. Among the persistent zonal asymmetries in Fig. 3 we recognize modes similar to the western Pacific and North Atlantic Oscillations (Wallace and Gutzler, 1981). Therefore, we conclude that the most persistent anomalies produced by the AC run have a realistic geographical pattern.

The 11 cases were selected on persistence over the area $\phi \geq 20°$N. Averaged over the same 11 cases, PC over the Southern Hemisphere was close to its normal value. In other words the persistent anomaly pattern that showed up in the mid- and high latitudes of the Northern Hemisphere were not part of a global locked-in mode.

d. Geographical distribution

The geographical distribution of autocorrelation can be studied suitably by employing a temporal correlation, TC, defined by (3). Figure 4 shows the zonal average of TC, as a function of latitude, for December to January for 700 mb height anomalies. The distribution of TC with latitude in the AC run (dashed line) is rather suggestive. At 50°S and 50°N, fast traveling cyclones dominate the entire spectrum and therefore TC is very low (5%). In the subtropics of both hemispheres, sluggish anticyclones increase month-to-month persistence. In the cold domes of air covering the poles the atmosphere is very stable and anomalies near the surface, once created, tend to persist a long time. Finally we note the complete lack of long time scales in 700 mb height anomalies over the region equatorward of 30°N (in December–January). These features are in almost complete disagreement with RW data (solid line, north of 15°N only). In the RW, autocorrelation seems to increase monotonically with decreasing latitude, reaching values as high as 60% at 15°N.

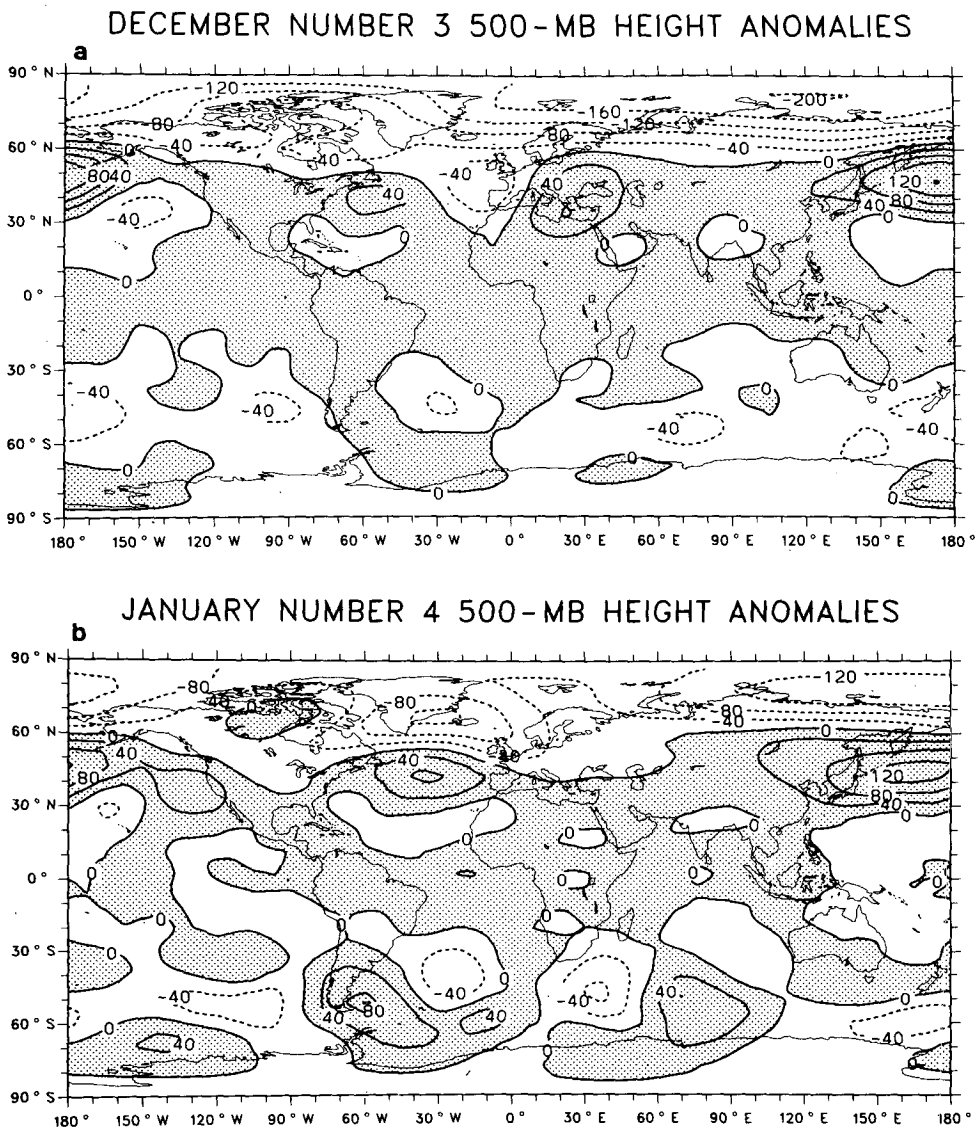

FIG. 3. The anomaly fields of the monthly mean 500-mb height occurring in (a) December of year 3 in the AC run, and (b) the adjacent January of year 4. The pattern correlation coefficient (in percentage) between these two maps, for the area $\phi \geq 20°$N, is 76; for the NH, SH and the whole globe this figure is 75, 17 and 64 respectively.

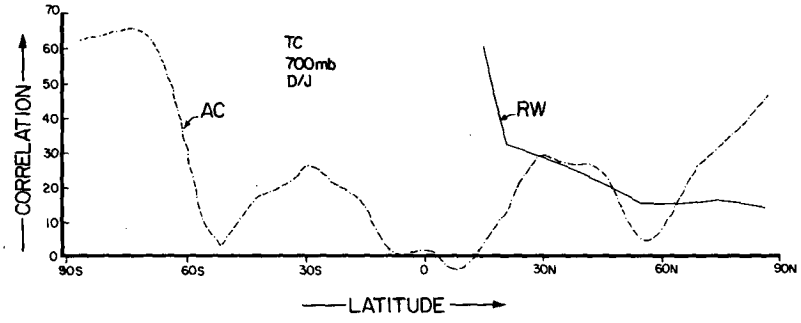

FIG. 4. The zonal average of the temporal December to January correlation (percentage) of anomalies in monthly mean 700 mb height fields as a function of latitude. In the AC run (dashed line) there are 20 Dec/Jan combinations, in the RW (solid line) 28.

The question is whether the differences in latitudinal distribution of TC between RW and AC have any physical implications. To some extent we might study here differences caused by artificial problems such as trends. The high autocorrelation near the poles in the AC run calls for an explanation. Either the dynamics in the polar region of the CCM are different from those in the RW or (contrary to expectation) interaction with the underlying surface decreases the lifetime of anomalies in the polar atmosphere of the real world. As to the high autocorrelation of the RW at latitudes south of 35°N it is worth mentioning that changes in observing and/or analyzing systems could easily introduce nonphysical low-frequency variability in RW data, especially in areas where the true interannual variability is low. Therefore, the high autocorrelation at low latitudes in the RW is somewhat suspect. To the extent that it is real, the interaction with the lower boundary seems a good candidate to explain high persistence in low latitudes. As we have seen in recent years (see Quiroz, 1983, for example) anomalies in various tropical circulation and Pacific SST indices are persistent over long periods of time, much more so than midlatitude height anomalies. This makes it qualitatively acceptable that autocorrelations in 700 mb height anomalies are relatively large in the low latitudes of the real world and low in the AC model.

e. Lags 2 and 3 months

In this section, we discuss the decay of autocorrelation in the AC run with increasing lag. The quantity selected is 700 mb height (since it has one of the highest one-month autocorrelation to start with). Table 5 shows average PCs in the area north of 20°N for all months, i.e., January/February, January/March, January/April, . . . etc., and yearly pooled PCs for lag 1, 2 and 3 months. The decrease of autocorrelation with lag is quite evident; the yearly pooled value at lag 2 is only 3.0. The decrease from 9.6 to 3.0 is somewhat slower than in a red noise process; in that case the yearly pooled autocorrelation at lags 2 and 3 would be 0.92 and 0.08, respectively. So there is some residual autocorrelation at large lags, the nature of which can be investigated better by using the TC.

Figure 5 shows the zonal average of TCs at lags 1, 2 and 3 months averaged over the year. In agreement with the results for PC, the lag 2 TC is generally much less than TC at lag 1, and there is no further decrease from lag 2 to lag 3. Spatially averaged TCs (over $\phi \geq 20°N$) are not much different from the PCs so the trend problem does not seem to be particularly large. Concentrating on $\phi \geq 20°N$, one can observe a somewhat erratic behavior of TC with latitude. There are areas where the lag 3 correlation is higher than the lag 2 correlation and close to the lag 1 correlation. In the Southern Hemisphere, the correlation decreases more regularly with lag, although slower than in a red noise process.

4. Conclusions and discussion

The primary aim of this study is to assess whether an interactive lower boundary has a substantial influence on the level of persistence of anomalies occurring in the earth's atmosphere. We measure persistence by calculating month-to-month correlation of large-scale anomalies appearing in monthly mean atmospheric fields. Here we compare month-to-month correlations in data generated by a general circulation model integration (in which the lower boundary is prescribed and going through 20 identical annual cycles) to similar calculations for the real world (RW). We realize that there may be more reasons for differences between AC and RW data than just a different treatment of the lower boundary. Nevertheless, we feel confident about three conclusions:

1) The level of month-to-month persistence in the RW over the extratropical Northern Hemisphere is somewhat higher than that in the AC, most convincingly so in the 500–1000 mb thickness field.

2) The largest differences occur in summer when the CCM, in the annual cycle mode, does not produce the summer maximum in persistence characteristic to the RW Northern Hemisphere extratropical circulation.

3) In spite of some small differences emphasized in conclusions 1 and 2, the most striking feature perhaps is that month-to-month persistence in extratropical RW and AC anomalies is generally at the same very low level.

The absence of a maximum in persistence of anomalies in summer in the AC run naturally leads to the ques-

TABLE 5. The average pattern correlation (%) of anomaly patterns in the 700 mb height over the area north of 20°N for lags of 1, 2 and 3 months in the AC run.

	Base month												
Lag	Jan*	Feb	Mar	Apr	May	Jun	Jul	Aug	Sep	Oct	Nov	Dec	Yr
1	16	9	8	14	6	4	5	11	11	7	5	19	9.6
2	12	−3	2	3	11	0	6	−2	1	4	−2	5	3.0
3	9	−2	−2	4	3	0	−3	−2	4	8	10	10	3.1

* 16, 12 and 9 give the correlation between January and February (16), January and March (12) and January and April (9), respectively.

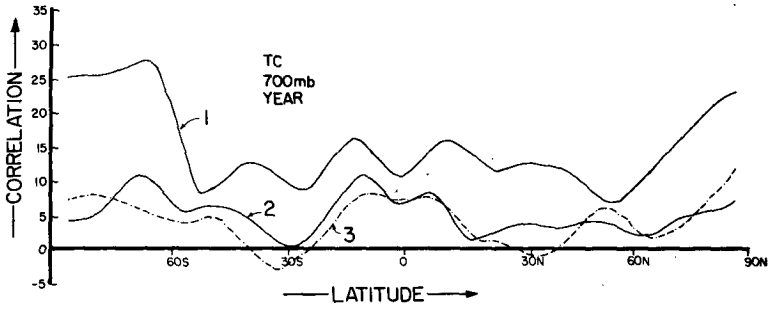

FIG. 5. As in Fig. 4 but for AC (700 mb height) at lags 1, 2 and 3 months, for yearly pooled calculations.

tion: What is missing in the model run, or present in the RW data that provides the maximum in persistence in summer in the RW? One may think here of feedback on soil moisture deficits over the continents which has been suggested by many workers (e.g., Namias, 1980) as the reason for persistent blocking events and associated heat waves in certain summers over the North American continent. Another possibility is that anomalies in forcing have a larger impact on the circulation in summer than in any other season. It is not too clear why this would be, although some speculations on this issue have been summarized by Haney (1984).

Our results concerning month-to-month persistence are consistent with Chervin (1986) who considered the interannual variability by comparing the variance of seasonal means in AC and RW. Chervin found that over the area $\phi \geq 20°N$, interannual variability of seasonal mean 700 mb and 1000 mb height is, in general, not higher in the RW than in the AC. This fits in quite well with our conclusion (based on the pattern correlation) that persistence in RW fields is not much higher than in AC's height fields.

To add credibility to the conclusion that RW and AC have nearly the same interannual variability in the Northern Hemisphere midlatitudes, Chervin (1986) made several additional extended CCM runs. In one of these runs, denoted here as ACVAR, the sea surface temperature went through the exact month-to-month evolution as observed during May 1958–April 1973 (Oort, 1983). Since the lower-boundary condition has interannual variability in this 15-year run (albeit, not interactive) one would expect the ACVAR run to resemble RW more closely than AC does. In fact, the month-to-month pattern correlation coefficients in ACVAR as a function of the time of the year are virtually indistinguishable from those presented in Fig. 1 for the AC experiment. Table 6 gives the average PC's for AC and ACVAR for all areas and all quantities considered. A parameter that has appreciably more persistence is the net energy transfer at the earth–atmosphere interface. This was to be expected. However, in the interior of the atmosphere the more persistent forcing anomalies at the lower boundary seem to have little or no impact, persistence in height and temperature fields in AC and ACVAR being very similar. In Table 7 we make a three-way comparison between AC, RW and ACVAR and it is clear that in the extratropics of the Northern Hemisphere, AC and ACVAR are much more close to each other (in terms of persistence of anomalies) than any of the two is to RW. Figure 6 (top) shows the zonally averaged TC at lag 1 month for 700 mb height anomalies in AC and ACVAR. As

TABLE 6. Pattern correlations (%) at 1 month lag for anomalies in monthly mean patterns of various quantities occurring in the AC and ACVAR runs. For each area and each quantity the average pattern correlation over 239 (AC) and 179 (ACVAR) month pairs is given. The results are for the whole year.

		Anomaly										
Area	Quantity	U3	T7	CUV3	CVT85	SU3	SV3	Z95	Z7	Z5	Z3	ENETS
Globe	AC	8.99	7.59	1.51	0.69	1.37	3.12	12.59	12.94	12.22	12.41	4.07
	ACVAR	11.80	8.94	1.48	0.88	2.81	2.96	13.00	11.79	10.81	12.50	9.76
$\phi \geq 20°N$	AC	8.02	7.85	0.67	1.25	0.89	3.69	8.56	9.55	9.43	9.68	4.48
	ACVAR	10.14	7.38	1.47	1.59	3.11	4.17	9.17	9.02	8.81	10.16	9.31
Northern Hemisphere	AC	8.04	8.23	0.72	1.17	0.99	3.07	9.45	10.04	9.54	10.31	3.98
	ACVAR	11.36	8.61	1.65	1.60	2.76	3.47	10.77	9.74	9.11	11.07	11.08
Southern Hemisphere	AC	9.50	6.68	2.56	0.75	1.79	3.14	14.78	14.92	13.94	13.74	3.73
	ACVAR	11.64	8.94	1.40	0.82	2.79	2.22	13.51	12.80	12.05	13.86	8.71

TABLE 7. Average pattern correlation for the area $\phi \geq 20°N$ at 1 month lag for the AC, the RW, and the ACVAR runs. Results are for the whole year.

	AC		RW		ACVAR	
Quantity	ave	sd	ave	sd	ave	sd
Z5	9.4	23	14.0	22	9.0	25
Z95 (P_{sl})	8.6	25	13.0	23	9.2	24
Z5–Z95 (Z5–Z10)	6.9	19	20.0	20	7.5	20
Total cases	239		342		179	

can be seen, the lifetime of anomalies in the tropical strip did increase substantially from AC to ACVAR but in the extratropics the effect of interannual variability in SST is not convincing. The increased persistence in Z7 anomalies in the tropical strip was not clearly visible in Table 6 because the interannual variability in Z7 in the tropics is so small compared to that in the extratropics (see bottom panel, Fig. 6). In summary, the comparison of AC and ACVAR does not contradict our earlier conclusion (no. 3) that interannual variability of the lower boundary does not increase substantially the lifetime of anomalies in midlatitudes.

We can offer only some speculation as to why the ACVAR results do not help at all to explain the small but significant differences between RW and AC (conclusions 1 and 2): (i) The atmospheric variability associated with interannual variability of the lower boundary is not additive to, but may be a substitute for natural variability of the midlatitude atmosphere. (ii) Using prescribed interannually varying SST is still a long way to go to a truly interactive lower boundary.

A possible explanation was advanced in Van den Dool (1983) for the observed level of and seasonality in month-to-month persistence of large-scale flow anomalies. In that paper, persistence was ascribed to steady anomalous forcing and the seasonality in persistence to the annual march of the background flow. The results of the present paper provide only partial support to reinforce Van den Dool's findings. In the AC model, we are sure that steady anomalous forcing is virtually absent. (We actually checked this by calculating the very low persistence of the anomalous energy flux at the surface and also calculating other forcings of the mean flow such as eddy fluxes. See Table 2.) If linear dynamic theory were valid and if the monthly mean atmosphere were in equilibrium with the anomalous forcing, we therefore expect persistence to be lower in AC than in RW. And, indeed, that is what we find, both on an annual mean and on a month-by-month (for temperature only) basis. The disagreement with Van den Dool (1983) is in the persistence in the AC model in the winter months (20%) which comes about without the various anomalous forcing

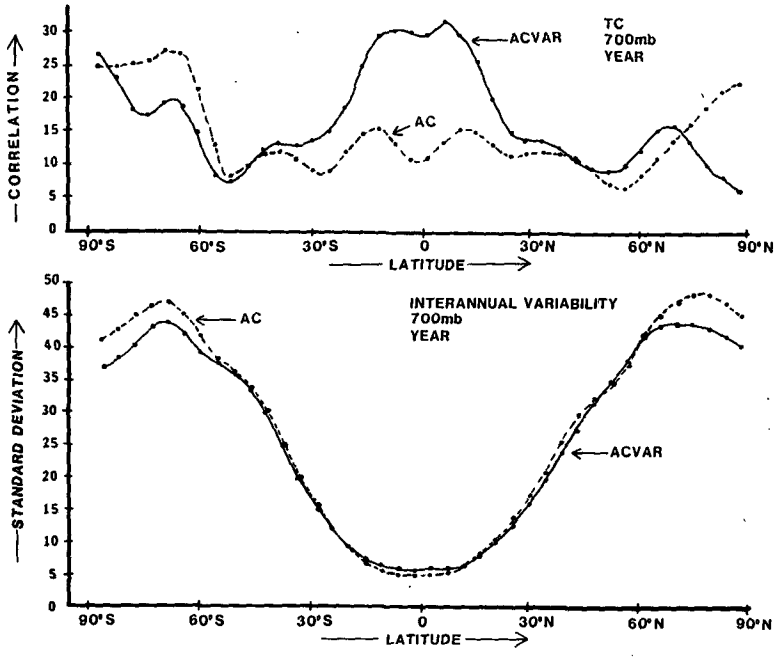

FIG. 6. Upper panel: the zonal average of the temporal month-to-month correlation coefficient (percentage) of anomalies in monthly mean 700 mb height fields as a function of latitude in the AC (dashed) and ACVAR (solid) run. Lower panel: the zonal average of the temporal standard deviation (gpm) of anomalies in monthly mean 700 mb height fields as a function of latitude in the AC (dashed) and ACVAR (solid) run. The results are in a yearly pooled data mode.

terms to be persistent. Apparently the internal dynamics can produce an appreciable amount of low-frequency variability in the winter-half year. This implies that the time-mean AC atmosphere is not quite in equilibrium with the anomalous forcing. In the winter months we might look upon the AC model as one of Brownian motion described by

$$\frac{d\bar{x}}{dt} = -\lambda\bar{x} + \epsilon$$

where $\bar{x}$ is monthly mean height, temperature or wind anomaly, and ϵ the forcing of monthly mean anomaly flow. Clearly, when $d\bar{x}/dt$ is small the response $\bar{x}$ has the same autocorrelation as ϵ (close to zero). This is apparently the case in summer. If $d\bar{x}/dt$ is nonnegligible the autocorrelation of $\bar{x}$ may be larger than that of ϵ (winter). In fact, we can evaluate in that case the feedback coefficient. On the assumption that ϵ has zero autocorrelation at lag 1 month, the feedback parameter is given by $\lambda = \ln(\overline{PC})/\text{month}$. Since $\overline{PC} \approx 0.20$, $\lambda \approx 6.10^{-7}$ sec^{-1}, or a damping time scale (working on height anomalies) of 15 days. This happens to be close to the coefficient for Rayleigh damping used in most linear modeling studies concerning stationary waves.

As a by-product of this study we have found that over the area north of 20°N there is good agreement in the spatial degrees of freedom (dof) in monthly mean height fields in RW and AC. (See Tables 2 and 4.) This means that the AC run produces anomalies that have about the right spatial scale. In fact the spatial dof for height fields is amazingly low and ranges (for $\phi \geq 20°$, 500 mb height) from 15 to 20 in winter to about 40 in summer. Further evidence of correct model behavior is that the most extreme individual cases of persistence are characterized by a strong zonally symmetric seesaw between the high and midlatitudes of the Northern Hemisphere, a feature also seen in the first empirical orthogonal function associated with winter mean 500 mb heights (Lau, 1981). So both in a statistical sense (dof) and in special cases the anomalies look quite realistic.

Acknowledgments. This work was started when the first author visited the National Center for Atmospheric Research. The support at NCAR, both scientifically and computationally, is gratefully acknowledged. The final product benefited from discussions with Grant Branstator, Alan Faller and Bob Livezey. This research was partially supported by the Climate Dynamics Program, Division of Atmospheric Sciences, National Science Foundation under Grant ATM-8314431.

REFERENCES

Blackmon, M. L., Y.-H. Lee and J. M. Wallace, 1984: Horizontal structure of 500 mb height fluctuations with long, intermediate and short time scales. *J. Atmos. Sci.*, **41**, 961–979.

Chervin, R. M., 1986: Interannual variability and seasonal climate predictability. *J. Atmos. Sci.*, **43**, 233–251.

Faller, A. J., 1981: An average correlation coefficient. *J. Appl. Meteor.*, **20**, 203–205.

Haney, R. L., 1984: Comment on "Seasonality in the association between surface temperatures over the United States and the North Pacific Ocean." *Mon. Wea. Rev.*, **112**, 868–870.

Horel, J. D., 1985: Persistence of the 500 mb height field during Northern Hemisphere winter. *Mon. Wea. Rev.*, **113**, 2030–2042.

Lau, N-C., 1981: A diagnostic study of recurrent meteorological anomalies appearing in a 15 year simulation with a GFDL general circulation model. *Mon. Wea. Rev.*, **109**, 2287–2311.

Livezey, R. E., and W. Y. Chen, 1983: Statistical field significance and its determination by Monte Carlo techniques. *Mon. Wea. Rev.*, **111**, 46–59.

Manabe, S., and D. G. Hahn, 1981: Simulation of atmospheric variability. *Mon. Wea. Rev.*, **109**, 2260–2286.

Namias, J., 1952: The annual course of month-to-month persistence of climatic anomalies. *Bull. Amer. Meteor. Soc.*, **33**, 279–285.

——, 1980: Severe drought and recent history. *J. Interdisciplinary History*, **X:4**, 697–712.

Oort, A. H., 1983: *Global Atmospheric Circulation Statistics, 1958–1973.* NOAA Prof. Pap. 14, U.S. Government Printing Office, Washington, D.C., 180 pp.

Opsteegh, J. D., and H. M. van den Dool, 1980: Seasonal differences in the stationary response of a linearized primitive equation model: Prospects for long-range weather forecasting? *J. Atmos. Sci.*, **37**, 2169–2185.

Panofsky, H. A., and G. W. Brier, 1968: *Some Applications of Statistics to Meteorology,* Pennsylvania State University Press, 224 pp.

Pitcher, E. J., R. C. Malone, V. Ramanathan, M. L. Blackmon, K. Puri and W. Bourke, 1983: January and July simulations with a spectral general circulation model. *J. Atmos. Sci.*, **40**, 580–604.

Quiroz, R. S., 1983: The climate of the "El Niño" winter of 1982–83—A season of extraordinary climatic anomalies. *Mon. Wea. Rev.*, **111**, 1685–1706.

Shukla, J., 1981: Dynamic predictability of monthly means. *J. Atmos. Sci.*, **38**, 2547–2572.

Simmons, A. J., J. M. Wallace and G. W. Branstator, 1983: Barotropic wave propagation and instability, and atmospheric teleconnection patterns. *J. Atmos. Sci.*, **40**, 1363–1392.

Van den Dool, H. M., 1983: A possible explanation of the observed persistence of monthly mean circulation anomalies. *Mon. Wea. Rev.*, **111**, 539–544.

——, and R. E. Livezey, 1984: Geographical distribution and seasonality of month-to-month correlation of monthly mean 700 mb heights. *Mon. Wea. Rev.*, **112**, 610–615.

Wallace, J. M., and D. S. Gutzler, 1981: Teleconnections in the geopotential height field during the Northern Hemisphere winter. *Mon. Wea. Rev.*, **109**, 784–812.